Supporting Information for

Formation of Monomeric Sn(II) and Sn(IV) Perfluoropinacolate Complexes and their Characterization by ^{119}Sn Mössbauer and ^{119}Sn NMR Spectroscopies

Jessica K. Elinburg,[a] Ariel S. Hyre,[a] James McNeely,[a] Todd M. Alam,[b] Steffen Klenner,[c] Rainer Pöttgen,[c] Arnold L. Rheingold,[d] and Linda H. Doerrer[a]

[a] Department of Chemistry, Boston University, 590 Commonwealth Avenue, Boston, MA 02215, USA. Email: doerrer@bu.edu.
[b] Department of Organic Material Science, Sandia National Laboratories, Albuquerque, NM 87185, USA.
[c] Institut für Anorganische und Analytische Chemie, Universität Münster, Corrensstrasse 30, D-48149 Münster, Germany.
[d] Department of Chemistry and Biochemistry, University of California, San Diego, 9500 Gilman Drive, MC 0332, La Jolla, CA 92093, USA.

Table of Contents

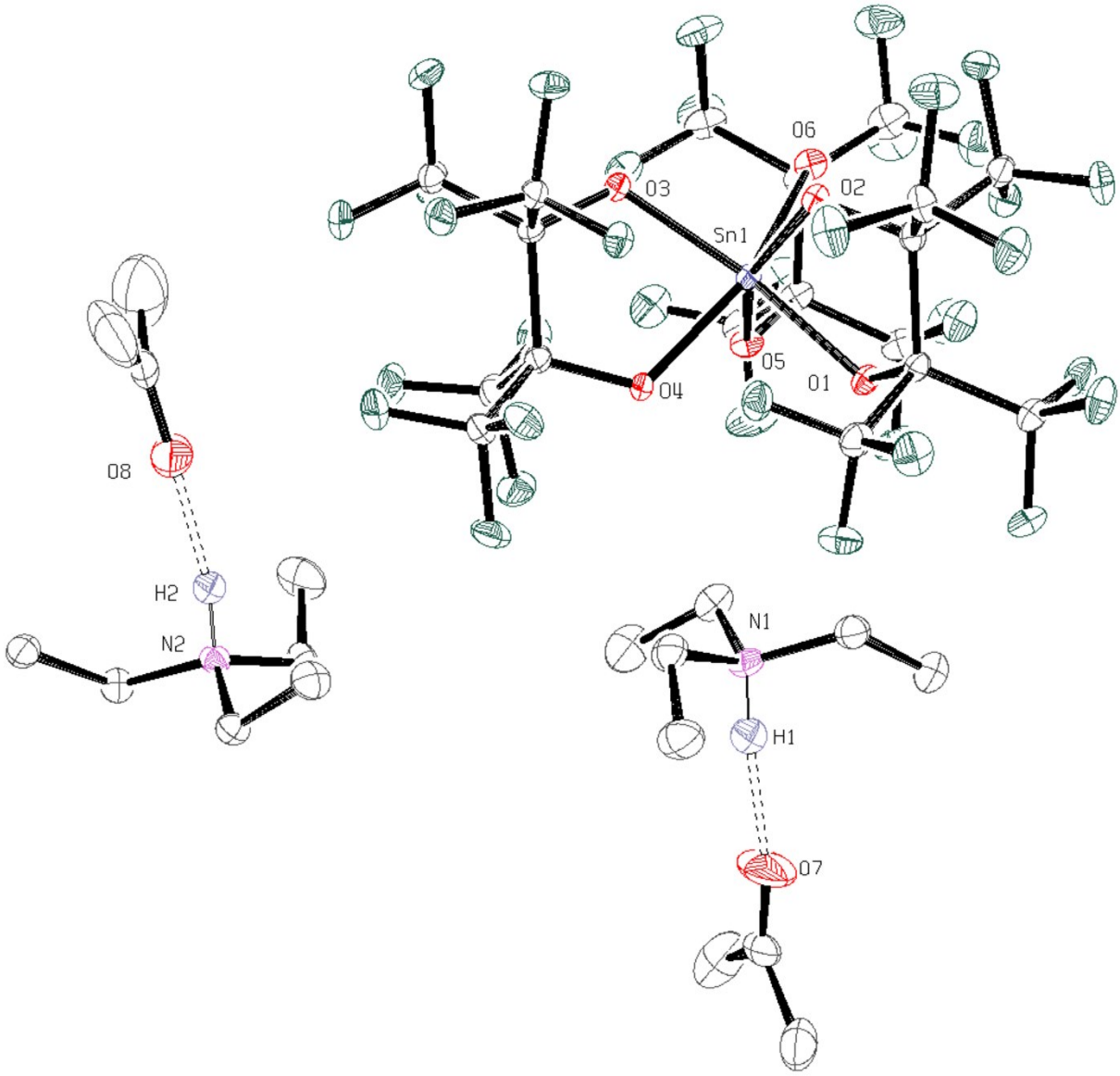

Figure S1. ORTEP of **1**. Ellipsoids shown at the 50% probability level. Hydrogen atoms, except those involved in hydrogen bonding, omitted for clarity.

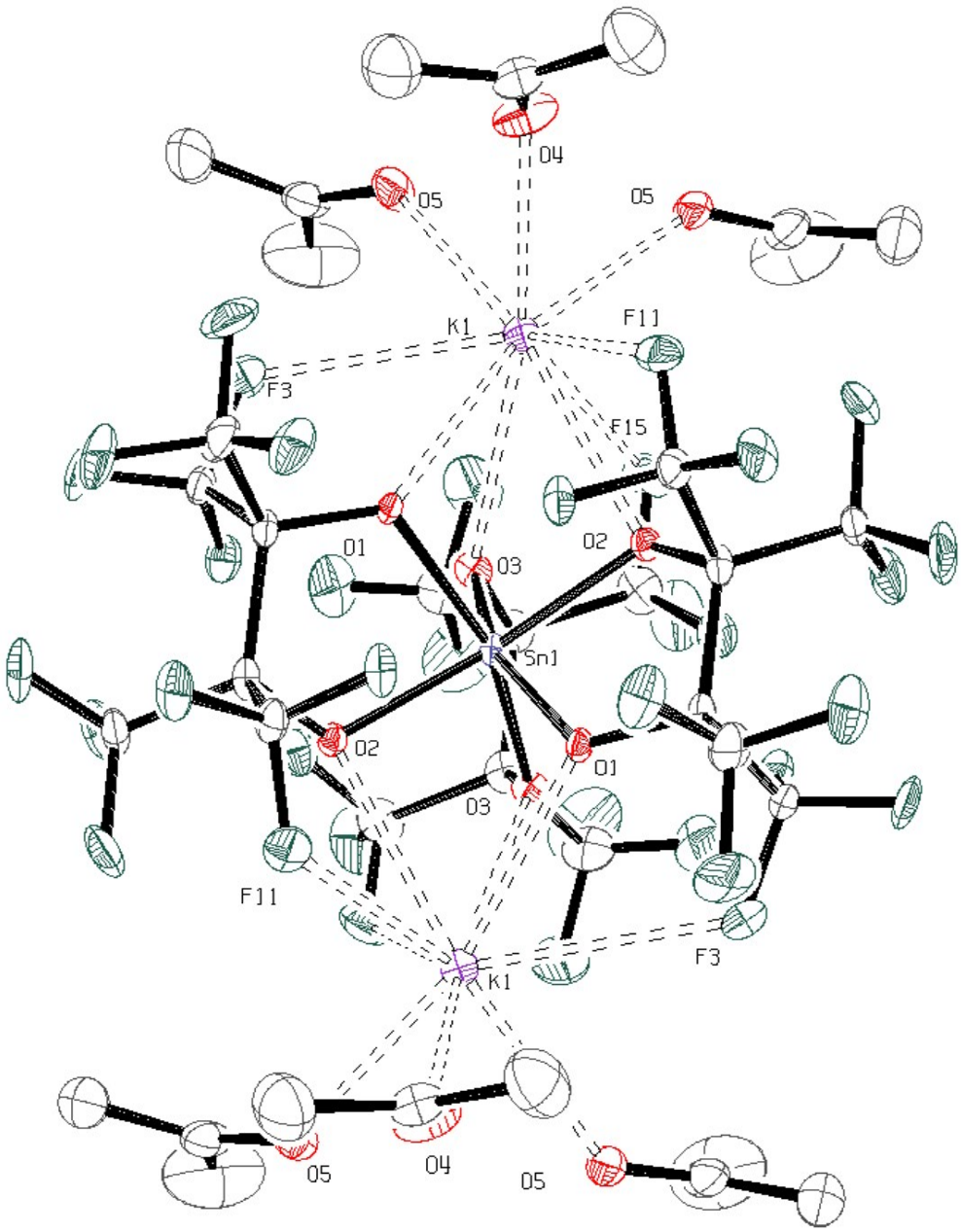

Figure S2. ORTEP of **2**. Ellipsoids shown at the 50% probability level. Hydrogen atoms omitted for clarity. $K_2[Sn(pin^F)_3]$ crystallizes with three equivalents of $(CH_3)_2CO$ per molecule (effectively 1.5/K^+); these solvent molecules are also bound to the K^+ counter ion of a neighboring Sn center in a repeating pattern. To show this pattern, the coordination of six $(CH_3)_2CO$ molecules is shown above.

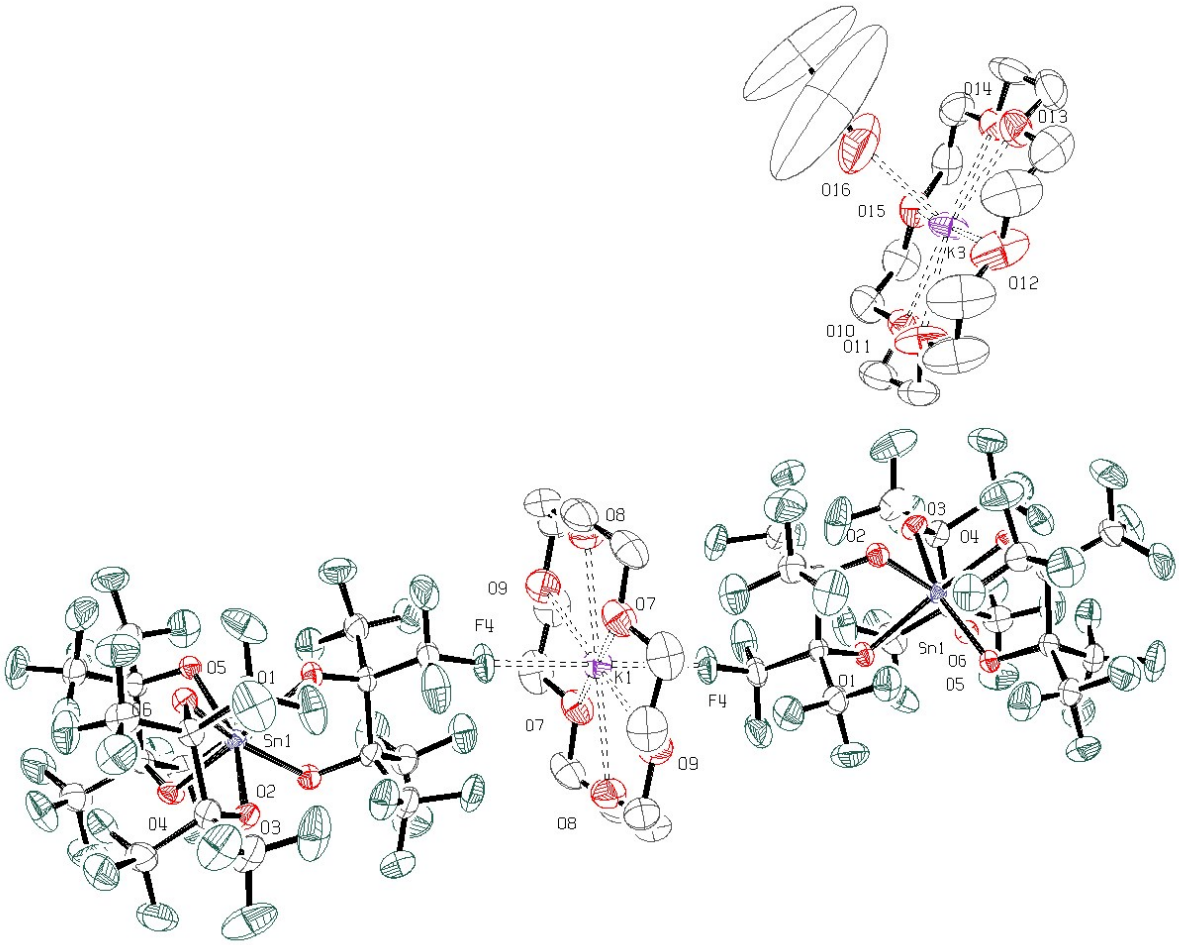

Figure S3. ORTEP of **3**. Ellipsoids shown at the 50% probability level. Hydrogen atoms omitted for clarity. $\{K(18C6)\}_2[Sn(pin^F)_3]$ crystallizes with a single equivalent of $(CH_3)_2CO$ per molecule, coordinated to one of the $\{K(18C6)\}^+$ counter ions; the other $\{K(18C6)\}^+$ moiety bridges two units of **3** via K···F interactions in a repeating pattern. To show these K···F interactions, two Sn(IV) centers of **3** are shown above.

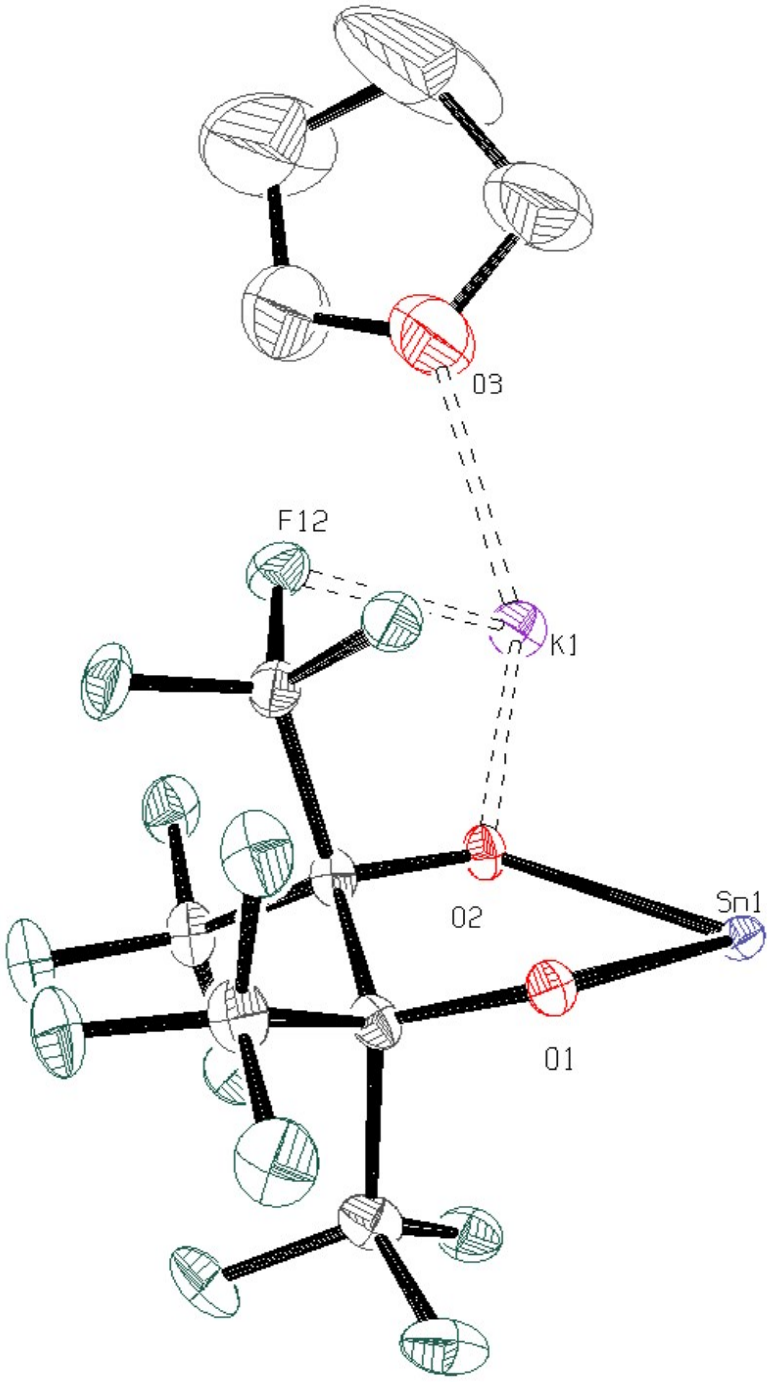

Figure S4. ORTEP of the asymmetric unit of **4**, which represents half of the $K_2[Sn(pin^F)_2]$ • 2 C_4H_8O moiety**.** Ellipsoids shown at the 50% probability level. Hydrogen atoms omitted for clarity.

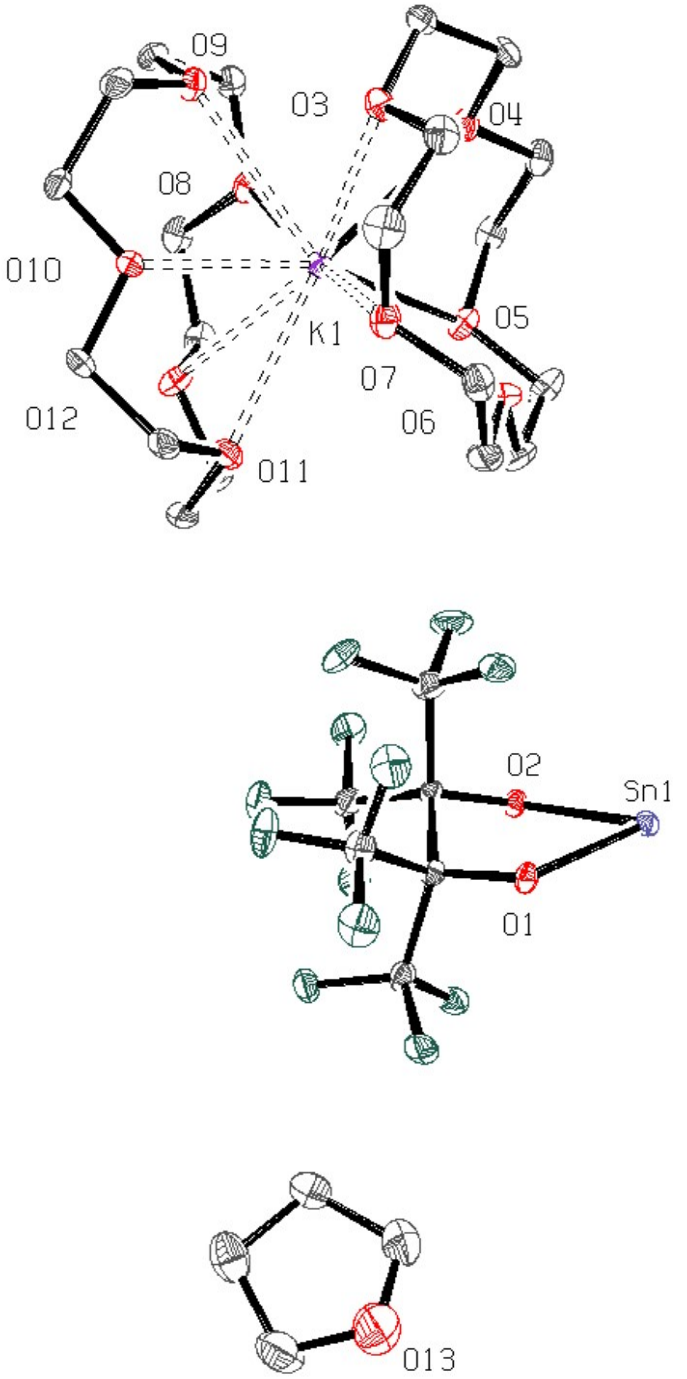

Figure S5. ORTEP of the asymmetric unit of **5**, which represents half of the symmetrical $\{K(15C5)\}_2[Sn(pin^F)_2] \bullet 2\ C_4H_8O$ unit**.** Ellipsoids shown at the 50% probability level. Hydrogen atoms omitted for clarity.

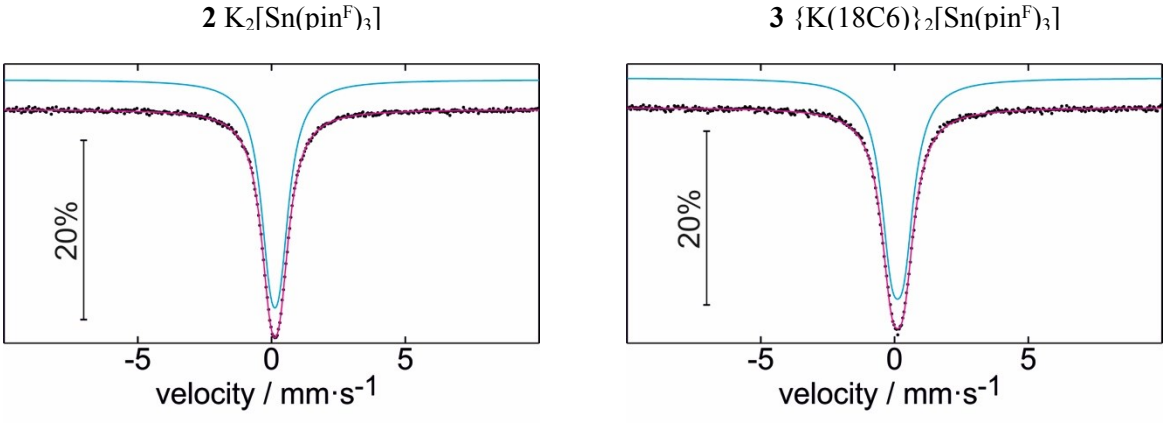

Figure S6. ^{119}Sn Mössbauer spectra of **2** and **3**.

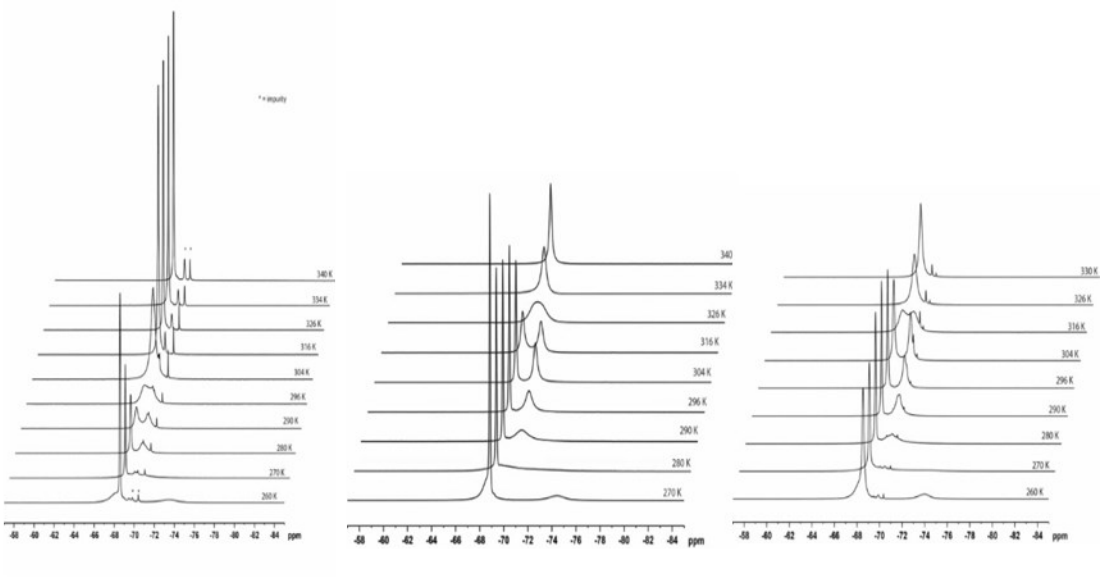

1 $[Et_3NH]_2[Sn(pin^F)_3]$ **2** $K_2[Sn(pin^F)_3]$ **3** $\{K(18C6)\}_2[Sn(pin^F)_3]$

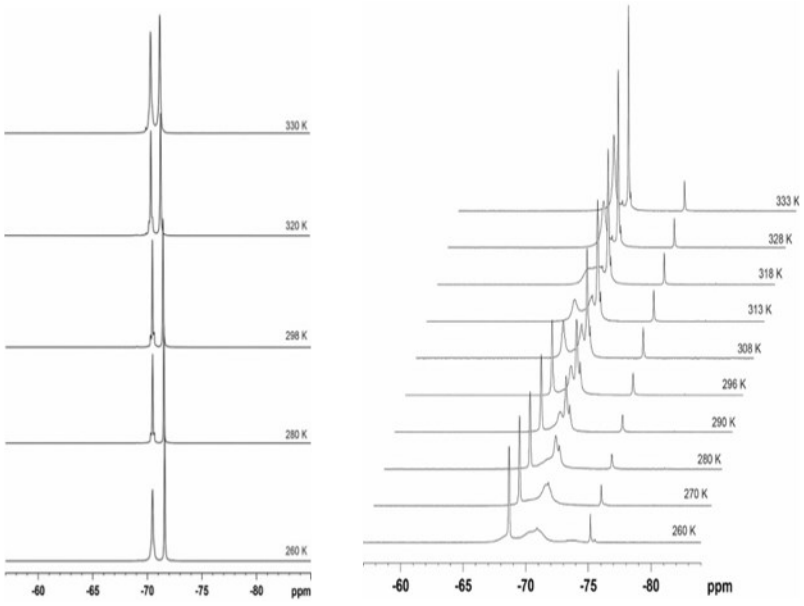

4 $K_2[Sn(pin^F)_2]$ **5** $\{K(15C5)\}_2[Sn(pin^F)_2]$

Figure S7. Variable temperature ^{19}F NMR data for **1-5.**

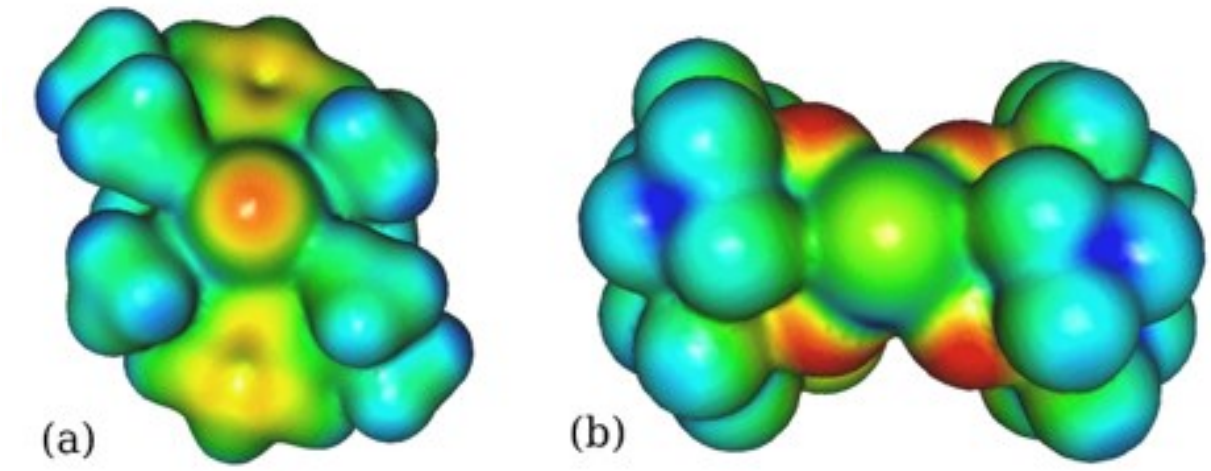

Figure S8. Electrostatic potential maps for $Sn[C_6H_3(NMe_2)_2\text{-}2,6]_2$ (−0.06 to 0.06) **(a)** and **5** (−0.17 to 0.28) **(b)**.

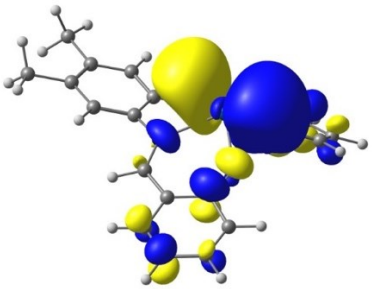

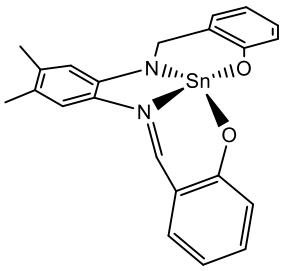

Vandenbergen et al.[1]

LUMO+7
E = 0.9323 eV

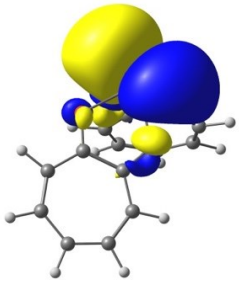

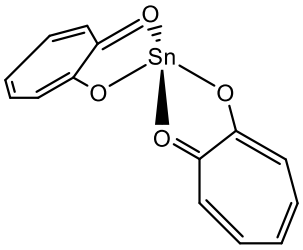

Barret et al.[2]

LUMO+4
E = 0.2025 eV

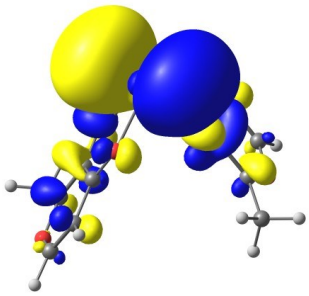

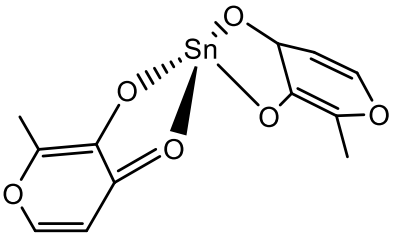

Barret et al.[2]

LUMO+4
E = 0.4725 eV

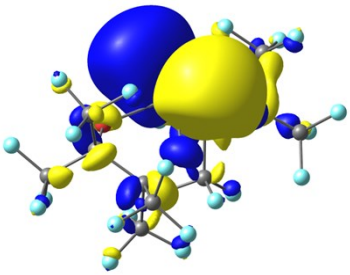

$[Sn(pin^{F})_2]^{2-}$

LUMO
E = 6.6683 eV

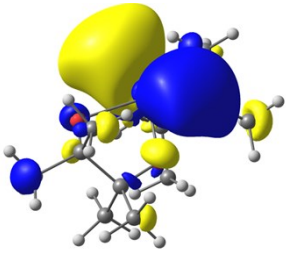

$[Sn(pin^{H})_2]^{2-}$

LUMO+3
E = 8.1256 eV

Figure S9. Calculated $5p_x$ (CMO) energies (TPSS0/cc-pwCVTZ(Sn)-DK/cc-pVTZ-DK/DKH) of four-coordinate Sn(II) complexes optimized at the TPSSh/DEF2-TZVP/RIJCOSX/D3BJ level.

Table S1. Crystallographic data collection and structure refinement parameters for **1-5**.

	1	**2**	**3**	**4**	**5**
	$[Et_3NH]_2[Sn(pin^F)_3]$ • 2 $(CH_3)_2CO$	$K_2[Sn(pin^F)_3]$ • 3 $(CH_3)_2CO$	$\{K(18C6)\}_2[Sn(pin^F)_3]$ • $(CH_3)_2CO$	$K_2[Sn(pin^F)_2]$ • 2 C_4H_8O	$\{K(15C5)_2\}_2[Sn(pin^F)_2]$ • 2 C_4H_8O
Empirical formula	$C_{36}H_{44}F_{36}N_2O_8Sn$	$C_{27}H_{18}F_{36}K_2O_9Sn$	$C_{39}H_{42}F_{36}K_2O_{16}Sn$	$C_{20}H_{16}F_{24}K_2O_6Sn$	$C_{60}H_{96}F_{24}K_2O_{26}Sn$
Formula weight	1435.42	1367.3	1647.61	1005.22	1886.25
Temperature (K)	100.0	100.0	100.0	100.0	100.0
Wavelength (Å)	0.71073	0.71073	0.71073	0.71073	0.71073
Crystal system	Triclinic	Orthorhombic	Triclinic	Monoclinic	Monoclinic
Space group	$P\bar{1}$	Pccn	$P\bar{1}$	$C2/c$	$C2/c$
a (Å)	12.3859(9)	10.869(2)	15.1378(16)	16.6806(14)	27.5254(11)
b (Å)	14.3035(11)	18.441(4)	16.2438(16)	12.1477(10)	10.7470(4)
c (Å)	15.7748(13)	21.954(4)	16.2454(16)	14.6638(13)	28.7368(15)
α (°)	82.239(2)	90	99.540(3)	90	90
β (°)	80.467(2)	90	114.932(3)	95.237(5)	114.007(2)
γ (°)	70.003(2)	90	112.822(3)	90	90
Volume (Å^3)	2580.6(3)	4400.4(14)	3068.9(5)	2958.9(4)	7765.4(6)
Z	2	4	2	4	4
Density (calculated) (g·cm^{-3})	1.85	2.06	1.78	2.26	1.61
Absorption coefficient (mm^{-1})	0.7	0.9	0.7	1.3	0.6
F(000)	1424	2656	1632	1952	3872
Crystal size mm^3	0.36 × 0.35 × 0.33	0.25 x 0.22 x 0.18	0.3 × 0.28 × 0.26	0.32 × 0.31 × 0.29	0.29 × 0.27 × 0.22

Theta range for data collection (°)	1.764 to 28.320	1.855 to 28.364	1.480 to 25.421	2.077 to 28.361	1.620 to 26.418
Index ranges	$-16 \le h \le 13$, $-19 \le k \le 15$, $-21 \le l \le 21$	-14<=h<=14, -13<=k<=24, -29<=l<=9	$-18 \le h \le 14$, $-19 \le k \le 19$, $-19 \le l \le 19$	$-22 \le h \le 17$, $-16 \le k \le 15$, $-19 \le l \le 16$	$-34 \le h \le 34$, $-12 \le k \le 13$, $-26 \le l \le 35$
Reflections collected	34045	20285	47361	11885	24929
Independent reflections	12802 [R_{int} = 0.0456]	5458 [R(int) = 0.0376]	11297 [R_{int} = 0.0331]	676 [R_{int} = 0.0648]	7963 [R_{int} = 0.0581]
Completeness to theta = 25.242°	99.9%	99.7 %	99.9%	99.7%	99.9%
Absorption correction	Semi-empirical from equivalents	Semi-empirical from equivalents	Semi-empirical from equivalents	Semi-empirical from equivalents	Semi-empirical from equivalents
Max. and min. transmission	0.563 and 0.519	0.563 and 0.511		0.746 and 0.683	0.745 and 0.695
Refinement method	Full-matrix least-squares on F^2	Full-matrix least-squares on F^2	Full-matrix least-squares on F^2	Full-matrix least-squares on F^2	Full-matrix least-squares on F^2
Data/parameters	12802/758	5458/343	11297/850	3676/240	7963/510
Goodness-of-fit on F^2	1.009	1.268	1.117	1.026	1.009
Final R indices [I > 2σ(I)]	$R1$ = 0.0378, $wR2$ = 0.0664	R1 = 0.0530, wR2 = 0.0921	$R1$ = 0.0413, $wR2$ = 0.1084	R1 = 0.0396, wR2 = 0.0932	$R1$ = 0.0389, $wR2$ = 0.0708
R indices (all data)	$R1$ = 0.0582, $wR2$ = 0.0734	R1 = 0.0715, wR2 = 0.0969	$R1$ = 0.0503, $wR2$ = 0.1146	R1 = 0.0511, wR2 = 0.1013	$R1$ = 0.0617, $wR2$ = 0.0783
Largest diff. peak and hole (e·Å^{-3})	0.62 and –0.70	0.991 and -0.566	1.60 and –0.48	0.75 and –0.84	0.42 and –0.55
SQUEEZE			Found: 35e/uc; calculated for acetone: 32e/uc		

Table S2. ^{119}Sn Moessbauer data plotted in Figure 3 in the main text.

Compound	CSD Code	Isomer Shift (δ, mm/s)	Quadrupole Splitting (ΔE_Q mm/s)	Reference
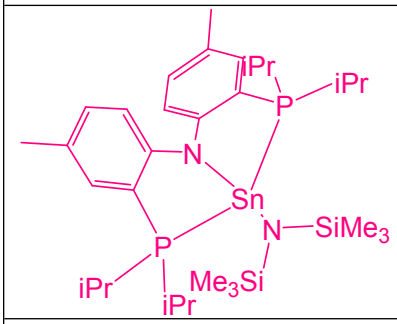	XAWFUY	2.779(4)	2.02(1)	3
[Sn{N(SiMe$_3$)$_2$}$_2$]	BUGROK	2.88	3.52	3
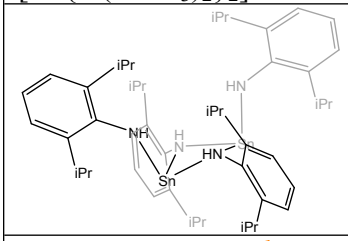	BOKBIN	2.884(13)	2.356(13)	4
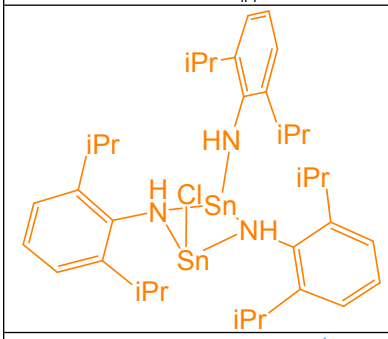	BOKBOT	3.222(10)	1.654(10)	4
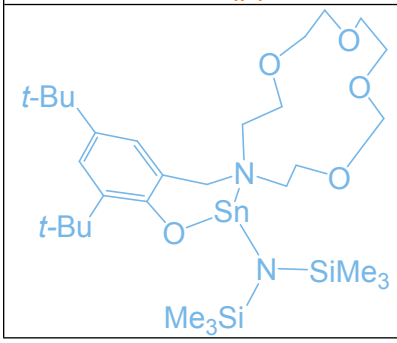	SASQUA	2.810 (5)	2.290 (8)	5

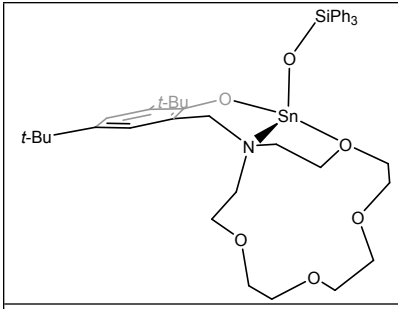	SASREL	2.849 (8)	2.09 (1)	5
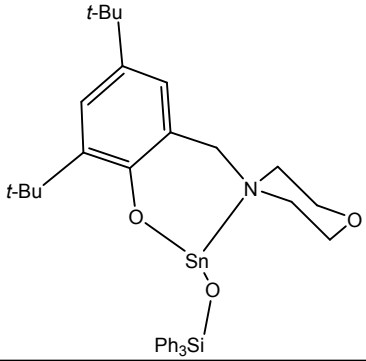	SASRAH	2.77 (1)	2.09 (2)	5
[Sn{N^O}][H_2N{$B(C_6F_5)_3$}$_2$]		3.37 (5)	1.91 (7)	
Ar'Sn-Sn{C_6H_3-2,6(C_6H_3-2,6-Pr^i_2)$_2$}	NEHTAW	2.658(2)	2.995(2)	6
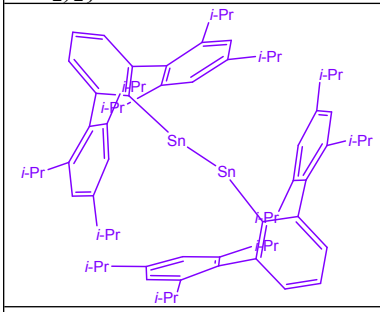	BAXSUO	2.69(3)	3.730(3)	6
[Cp_2Sn]	BAHJAV	3.73	0.65	7
[Cp^*_2Sn]	MCYPSN	3.83	0	8
[$Sn(C_7H_8)_3$]$^{2+}$[$B(C_6F_5)_4$]$_2$	IZUXAD	4.14(1)	0.38(3)	9

Computational details. All calculations described in the following were performed with the ORCA electronic structure package.[10-12] Any calculations performed with another package are described in the main text. In the tables that follow, the calibration of the different theoretical models is described and the preformance of the models with respect to duplicating the experimental quadrupolar splitting is shown. The calibration was done against the set described by Barone et al.[13-15] Geometries were optmized at the BP86[16, 17]/DEF2-SV(P) [18, 19]/D3BJ[20, 21] and TPSSh[22]/DEF2-TZVP/D3BJ/RIJCOSX[23-25] levels. Experimental geometries were modified by optimizing the hydrogen positions at the BP86/DEF2-SV(P)/D3BJ level. In All other relevant details are shown in the main text or the footnotes of the tables.

Table S3. Summary of correlation plots of exp. |ΔE| (mm s^{-1}) vs. calc. values of |V| (a.u.).

Method	Basis Set	Structure	Slope	SE	Intercept	SE	R^2
BP86	DKH-TZVPP[iv]	BP86[i]	0.7280	0.045	0.08129	0.163	0.889
TPSSh	DKH-TZVPP[iv]	TPSSh[ii]	0.7216	0.045	0.07969	0.166	0.886
TPSS0[26]	DKH-TZVPP[iv]	TPSSh[ii]	0.6744	0.041	0.08801	0.161	0.892
TPSSh	DKH-TZVPP[iv]	Expt.[iii]	0.7217	0.033	-0.04064	0.125	0.938
TPSS0	DKH-TZVPP[iv]	Expt.[iii]	0.6751	0.030	-0.03725	0.119	0.943
TPSS0	cc-pwCVTZ-DK[v]	TPSSh[ii]	0.6909	0.041	0.05123	0.159	0.897
TPSS0	cc-pwCVTZ-DK[v]	Expt.[iii]	0.6885	0.030	-0.05976	0.119	0.944
MP2[vi]	cc-pwCVTZ-DK[v]	Expt.[iii]	0.6474	0.023	0.02941	0.092	0.964
CCSD(T)[vii]	cc-pwCVTZ-DK[v]	Expt.[iii]	0.5673	0.023	0.00261	0.107	0.952

i. BP86/DEF2-SV(P)/D3BJ
ii. TPSSh/DEF2-TZVP/D3BJ/RIJCOSX
iii. Hydrogens optimized at the BP86/DEF2-SV(P)/D3BJ level.
iv. In ORCA parlance, this is the old-DKH-TZVPP[27] basis set.
v. Sn atoms modeled with cc-pwCVTZ-DK[28], all other atoms modeled with cc-pVTZ-DK[29].
vi. Energies evaluated with Grimme's SCS-MP2[30] with RI approximation using the CC-PVTZ/C[31] auxiliary basis set for non-tin atoms, and ORCA's AutoAux[32] routine for Sn. Relaxed densities were used.
vii. DLPNO-CCSD(T) with unrelaxed densities. Normal PNO thresholds were used.

Table S4. Summary of model performance.

Method	Basis Set	Structure	$K(THF)_2[Sn^{II}(pin^F)_2]$	$[Sn^{II}(pin^F)_2]^{2-}$	Δ
Expt.	-	-	1.698	2.153	0.455
TPSSh	DKH-TZVPP	TPSSh	1.813	1.851	0.038
TPSS0	DKH-TZVPP	TPSSh	1.817	1.824	0.007
TPSSh	DKH-TZVPP	Expt.	1.868	1.930	0.062
TPSS0	DKH-TZVPP	Expt.	1.846	1.925	0.079
TPSS0	cc-pwCVTZ-DK	Expt.	1.849	1.940	0.091
MP2	cc-pwCVTZ-DK	Expt.	1.639	1.785	0.146
CCSD(T)	cc-pwCVTZ-DK	Expt.	1.746	1.853	0.107

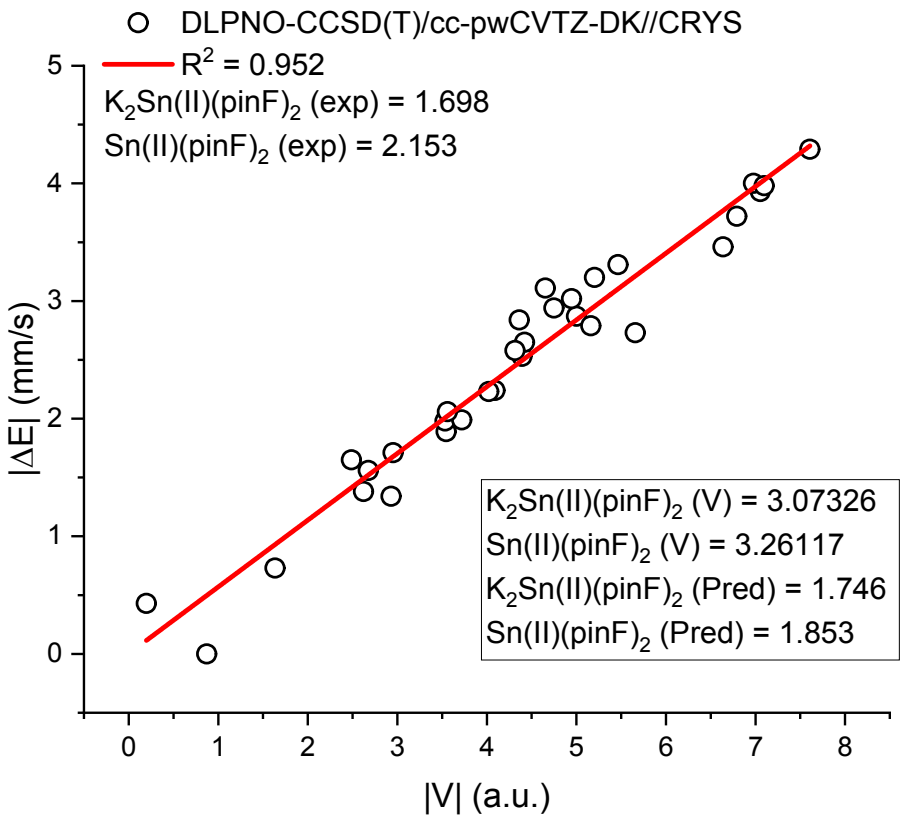

Figure S10. Calibration curve for DLPNO-CCSD/cc-pwCVTZ-DK(Sn)/cc-pVTZ-DK/DKH/RIJCOSX/AutoAux//Expt.

References:

1. A. M. Vandenbergen, J. D. Cashion, G. D. Fallon and B. O. West, *Aust. J. Chem.*, 1990, **43**, 1559-1571.
2. M. C. Barret, M. F. Mahon, K. C. Molloy, J. W. Steed and P. Wright, *Inorg. Chem.*, 2001, **40**, 4384-4388.
3. J. Henning, H. Schubert, K. Eichele, F. Winter, R. Poettgen, H. A. Mayer and L. Wesemann, *Inorg. Chem.*, 2012, **51**, 5787-5794.
4. W. A. Merrill, J. Steiner, A. Betzer, I. Nowik, R. Herber and P. P. Power, *Dalton Trans.*, 2008, DOI: 10.1039/b809671f, 5905-5910.
5. V. Poirier, T. Roisnel, S. Sinbandhit, M. Bochmann, J.-F. Carpentier and Y. Sarazin, *Chem. - Eur. J.*, 2012, **18**, 2998-3013, S2998/2991-S2998/2921.
6. G. H. Spikes, J. R. Giuliani, M. P. Augustine, I. Nowik, R. H. Herber and P. P. Power, *Inorg. Chem.*, 2006, **45**, 9132-9136.
7. R. L. Williamson and M. B. Hall, *Organometallics*, 1986, **5**, 2142-2143.
8. M. J. Heeg, C. Janiak and J. J. Zuckerman, *J. Am. Chem. Soc.*, 1984, **106**, 4259-4261.
9. A. Schaefer, F. Winter, W. Saak, D. Haase, R. Poettgen and T. Mueller, *Chem. - Eur. J.*, 2011, **17**, 10979-10984, S10979/10971-S10979/10912.
10. F. Neese, *Wiley Interdiscip. Rev. Comput. Mol. Sci.*, 2012, **2**, 73-78.
11. F. Neese, *Max Planck Institute for Chemical Energy Conversion: Mülheim a. d. Rurh, Germany*, 2017.
12. F. Neese, *Wiley Interdiscip. Rev. Comput. Mol. Sci.*, 2018, **8**, e1327.
13. G. Barone, A. Silvestri, G. Ruisi and G. L. Manna, *Chem. Eur. J.*, 2005, **11**, 6185-6191.
14. G. Barone, R. Mastalerz, M. Reiher and R. Lindh, *J. Phys. Chem. A*, 2008, **112**, 1666-1672.
15. J. W. Krogh, G. Barone and R. Lindh, *Chemistry*, 2006, **12**, 5116-5121.
16. A. D. Becke, *Phys. Rev. A*, 1988, **38**, 3098-3100.
17. J. P. Perdew, *Phys. Rev. B*, 1986, **33**, 8822-8824.
18. F. Weigend and R. Ahlrichs, *Physical Chemistry Chemical Physics*, 2005, **7**, 3297-3305.
19. F. Weigend, *Physical Chemistry Chemical Physics*, 2006, **8**, 1057-1065.
20. S. Grimme, J. Antony, S. Ehrlich and H. Krieg, *J. Chem. Phys.*, 2010, **132**, 154104.
21. S. Grimme, S. Ehrlich and L. Goerigk, *J. Comput. Chem.*, 2011, **32**, 1456-1465.
22. J. Tao, J. P. Perdew, V. N. Staroverov and G. E. Scuseria, *Phys. Rev. Lett.*, 2003, **91**, 146401.
23. D. Ganyushin, N. Gilka, P. R. Taylor, C. M. Marian and F. Neese, *J. Chem. Phys.*, 2010, **132**, 144111.
24. S. Kossmann and F. Neese, *Chem. Phys. Lett.*, 2009, **481**, 240-243.
25. F. Neese, F. Wennmohs, A. Hansen and U. Becker, *Chem. Phys.*, 2009, **356**, 98-109.
26. S. Grimme, *J. Phys. Chem.*, 2005, **109**, 3067-3077.
27. D. A. Pantazis, X. Y. Chen, C. R. Landis and F. Neese, *J. Chem. Theory Comput.*, 2008, **4**, 908-919.
28. D. H. Bross and K. A. Peterson, *Theor. Chem. Acc.*, 2013, **133**, 1434.
29. W. A. d. Jong, R. J. Harrison and D. A. Dixon, *J. Chem. Phys.*, 2001, **114**, 48-53.
30. S. Grimme, *J. Chem. Phys.*, 2003, **118**, 9095-9102.
31. F. Weigend, A. Köhn and C. Hättig, *J. Chem. Phys.*, 2002, **116**, 3175-3183.

32. G. L. Stoychev, A. A. Auer and F. Neese, *J. Chem. Theory Comput.*, 2017, **13**, 554-562.